Fisheries bycatch risk to marine megafauna is intensified in Lagrangian coherent structures

Kylie L. Scales[a,b,1], Elliott L. Hazen[b], Michael G. Jacox[b,c], Frederic Castruccio[d], Sara M. Maxwell[e], Rebecca L. Lewison[f], and Steven J. Bograd[b]

[a]School of Science and Engineering, University of the Sunshine Coast, Maroochydore, QLD 4556, Australia; [b]Environmental Research Division, National Oceanic and Atmospheric Administration Southwest Fisheries Science Center, Monterey, CA 93940; [c]Physical Sciences Division, National Oceanic and Atmospheric Administration Earth System Research Laboratory, Boulder, CO 80305; [d]Climate and Global Dynamics Laboratory, National Center for Atmospheric Research, Boulder, CO 80305; [e]Department of Biological Sciences, Old Dominion University, Norfolk, VA 23529; and [f]Institute for Ecological Monitoring and Management, San Diego State University, San Diego, CA 92812

Edited by Alistair Hobday, Commonwealth Scientific and Industrial Research Organization, and accepted by Editorial Board Member David W. Schindler May 22, 2018 (received for review January 23, 2018)

Incidental catch of nontarget species (bycatch) is a major barrier to ecological and economic sustainability in marine capture fisheries. Key to mitigating bycatch is an understanding of the habitat requirements of target and nontarget species and the influence of heterogeneity and variability in the dynamic marine environment. While patterns of overlap among marine capture fisheries and habitats of a taxonomically diverse range of marine vertebrates have been reported, a mechanistic understanding of the real-time physical drivers of bycatch events is lacking. Moving from describing patterns toward understanding processes, we apply a Lagrangian analysis to a high-resolution ocean model output to elucidate the fundamental mechanisms that drive fisheries interactions. We find that the likelihood of marine megafauna bycatch is intensified in attracting Lagrangian coherent structures associated with submesoscale and mesoscale filaments, fronts, and eddies. These results highlight how the real-time tracking of dynamic structures in the oceans can support fisheries sustainability and advance ecosystem-based management.

ocean model | marine vertebrate | gillnet | Finite-Time Lyapunov Exponent | fronts

Managing the competing demands of resource extraction and biodiversity conservation is a central challenge in maintaining ecosystem function across terrestrial and marine systems (1, 2). In the oceans, overharvesting, habitat degradation, and bycatch—incidental catch that is unwanted, unused, or unmanaged (3)—are global-scale barriers to fisheries sustainability. Seafood is a major protein source for more than 3 billion humans worldwide (4), and the importance of a sustainable supply will increase with the rapidly rising global population (5). Prioritizing the ecological sustainability of marine fisheries is crucial to preventing ecosystem collapse and protecting food sources and future livelihoods in fisheries-reliant communities (6, 7).

Nontarget catch represents an estimated 40% by mass of all marine catch (3) and has been identified as the most serious global threat to a diverse array of marine vertebrates including sea turtles, seabirds, marine mammals, pinnipeds, and elasmobranchs (3, 8–10). Marine megafauna populations face a range of cumulative anthropogenic stressors, particularly in coastal zones under intensive human use (11), and many are of immediate conservation concern (12–14). Life history characteristics such as long life span, low fecundity, late maturity, and wide-ranging movements exacerbate the ecological impacts of fisheries bycatch, as populations struggle to buffer anthropogenic pressure. The removal of high-trophic level species, described as trophic downgrading (15, 16), causes substantial changes in ecosystem function (12) and reduces the profitability of fisheries (5).

To halt or reverse these trends, bycatch mitigation measures such as changes to fishing gear and practice and fishing effort reallocation and redistribution have been successfully implemented in many fisheries (17, 18). However, the relative success of these mitigation options relies upon management effort being both well-targeted in space and time, and effectively enforced. Spatial fisheries management solutions, such as Marine Protected Areas, time-area closures, or gear modification zones, require a scale-matched understanding of the spatiotemporal dynamics of fisheries and of the habitat preferences of both target species and bycatch-sensitive populations.

Bycatch hotspots and trends have been explored using spatially and temporally explicit fisheries data at global (9, 10, 19–21), ocean-basin (22–24), national (25, 26), and regional (27, 28) scales. However, previous studies have predominantly focused on correlations and long-term patterns of spatiotemporal overlap among fisheries and high-use habitats of marine vertebrates (23, 24, 29) and are often population—or species—specific. While these studies have yielded important insights into the location of bycatch hotspots, seldom do the analytical techniques used account for spatiotemporal dynamics, yield insights at management-relevant spatial (kilometers to tens of kilometers) or temporal (daily, weekly, monthly) scales, or attempt to identify the fundamental physical drivers that underlie observed patterns.

It is well-established that biophysical coupling at submesoscale and mesoscale [hereafter (sub)mesoscale] features such as frontal systems and eddies can result in productive foraging habitats for marine predators (29–32). Fronts, eddies, and filaments can become hotspots of productivity through nutrient enrichment, turbulent

Significance

Marine capture fisheries provide a valuable source of protein and are economically important in coastal communities. However, fisheries sustainability is impacted by incidental capture of nontarget species (bycatch), which remains a major global threat to marine megafauna such as sharks, sea turtles, seals, cetaceans, and seabirds. Understanding where and when bycatch events take place can guide fisheries sustainability solutions. Here, we model how dynamic structures in the ocean such as fronts and eddies influence fisheries effort, catch, and bycatch likelihood. We find that bycatch of a diverse range of species is more likely in attracting Lagrangian coherent structures, in which water masses meet and aggregate prey, predators, and fishers into hotspots of risk.

Author contributions: K.L.S., E.L.H., and S.J.B. designed research; K.L.S. performed research; M.G.J., F.C., S.M.M., and R.L.L. contributed data; K.L.S. analyzed data; and K.L.S., E.L.H., M.G.J., F.C., S.M.M., R.L.L., and S.J.B. wrote the paper.

The authors declare no conflict of interest.

This article is a PNAS Direct Submission. A.H. is a guest editor invited by the Editorial Board.

[1]To whom correspondence should be addressed. Email: kscales@usc.edu.au.

This article contains supporting information online at www.pnas.org/lookup/suppl/doi:10.1073/pnas.1801270115/-/DCSupplemental.

Published online June 25, 2018.

vertical mixing (33, 34), proliferation of phytoplankton, and physical aggregation of zooplankton (35). These processes of biophysical coupling attract midlevel consumers such as small pelagic fish and gelatinous zooplankton, which are themselves prey items for marine megafauna such as seabirds, turtles, cetaceans, pinnipeds, sharks, and large teleost fishes. Marine predators of multiple taxa are known to exploit these accessible and predictable foraging opportunities (32, 36, 37), as are the fisheries that target both bait fish and large predatory teleosts that are found in higher numbers in association with submesoscale structures (38). Hence, (sub)mesoscale structures can concentrate forage resources, fish, fisheries, and predators into hotspots of bycatch risk to marine vertebrates.

Broad-scale regions of increased fisheries bycatch risk have been identified using overlap-based analyses that map oceanic structures using common remotely sensed measures of the physical environment such as sea surface temperature (SST) and surface chlorophyll-a concentration (23, 24, 28, 39–41). Front frequency and frontal probability indices have highlighted broad-scale regions of persistent frontal activity as core foraging habitats of marine megafauna, and hotspots of fisheries overlap (29), but are more useful for identifying patterns over seasonal, annual, or climatological scales than for resolving real-time interactions. Time-matched remotely sensed data have been used to examine correlations among catch rates of key targeted species (e.g., tuna and billfish) and contemporaneous mesoscale structures, using SST, chlorophyll-a, and sea level anomalies (SLA) (42–44). Satellite tracking studies have related animal movements to thermal fronts in SST fields, or chlorophyll-a fronts in ocean color fields, through the derivation of gradient-based metrics (45), spatial SD, or histogram-based edge detection (46). While these techniques have advanced our understanding of structure and function in pelagic systems, they cannot adequately resolve the influence of the dynamic submesoscale flow field in driving real-time fisheries interactions. Objective validation of the functional responses of marine predators, and of fisheries, to dynamic structures is complex and reliant on acquisition of data at sufficient scales to link pattern and process (47).

An alternative technique is to use Lagrangian methods to identify dynamic structures in ocean surface velocity fields. For example, the Finite-Time or Finite-Size Lyapunov Exponents [FT(S)LE] can be applied to sequences of surface velocity fields to identify Lagrangian coherent structures (LCS) in the surface flow (48). LCS are material curves that map dynamic flow features (49) and are known to contribute to the structuring of marine ecosystems (50). LCS mapping identifies attracting structures in the surface flow field using ridges in backward-in-time FT(S)LE and repelling structures using forward-in-time FT(S)LE. LCS mapping is emerging as a powerful technique in marine spatial ecology and has been used to identify habitats of marine predators such as seals (37, 51), seabirds (52), and baleen whales (36, 53) and to evaluate the design of Marine Protected Areas (54). However, FSLE derived from satellite altimetry fields is served only as a coarse resolution (0.25°), 3-d composite, limiting its utility for inferring real-time mechanistic linkages. The periodicity of satellite overpasses (1 wk to 10 d) can result in over-smoothing in the velocity field defined through altimetry, reducing the temporal and spatial resolution in the resultant FSLE product, and satellite altimetry can exhibit lower performance in upwelling regions, such as the California Current System (CCS), than elsewhere.

Here, we present a high-resolution LCS mapping product derived from daily velocity fields of a data assimilative CCS configuration of the Regional Ocean Modeling System (ROMS). We take a detailed, multispecies approach to quantifying the influence of the dynamic physical environment on the likelihood of marine megafauna bycatch in the CCS. Seasonal wind-driven upwelling in the CCS, a global marine biodiversity hotspot, results in the development of rich feeding grounds that support vast numbers of marine vertebrates, both migrant and resident (39), many of which are protected under international and US federal legislation (Marine Mammal Protection Act 1972; Endangered Species Act 1973). The CCS is a highly energetic eastern boundary upwelling system with a complex, dynamic flow field characterized at the submesoscale by fronts, eddies, and filaments. Using a spatially explicit time series (1990–2010) of National Oceanic and Atmospheric Administration (NOAA) fisheries observer data from a drift gillnet fishery, coupled with high-resolution FTLE fields derived from ROMS, we explore how attracting LCS influence the likelihood of fisheries interactions with both exploited and protected marine megafauna.

Results

Attracting LCS, and the spatiotemporal evolution of these convoluted and dynamic features, were mapped daily over the CCS domain for the period 1990–2010 (Fig. 1). Our findings demonstrate that over the 21-y period examined, fisheries effort in the California drift gillnet fishery was significantly more likely to be associated with increased magnitude of FTLE, establishing that this fishery targets attracting LCS associated with (sub)mesoscale surface structures such as upwelling filaments, fronts, and eddies. The locations of gillnet sets on haul-out were more likely than unfished locations to be associated with attracting LCS (as indicated by the median FTLE magnitude; see *Methods*). The slope of the relationship between the probability of fishing vessel presence and the strength of the attracting LCS field was highly significant in all model iterations (*SI Appendix*).

The primary target species of this drift gillnet fishery is broadbill swordfish *Xiphias gladius*. Several secondary target species are incidentally caught yet retained for sale (e.g., Pacific bluefin tuna *Thunnus orientalis*, pelagic thresher shark *Alopias pelagicus*, common thresher shark *Alopias vulpinus*, shortfin mako shark *Isurus oxyrinchus*, smooth hammerhead shark *Sphyrna zygaena*, opah *Lampris guttatus*), and a range of nontarget species are caught as bycatch (e.g., blue shark *Prionace glauca*, ocean sunfish *Mola mola*, leatherback turtle *Dermochelys coriacea*, loggerhead turtle *Caretta*

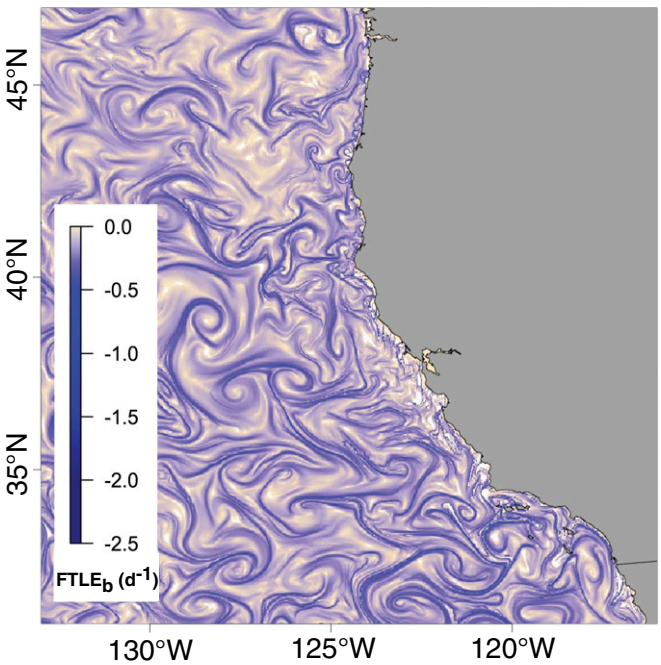

Fig. 1. Attracting LCS in the California Current System, mapped as a daily field using FTLE$_b$ applied to zonal and meridional velocity fields from California Current configuration of the ROMS (65).

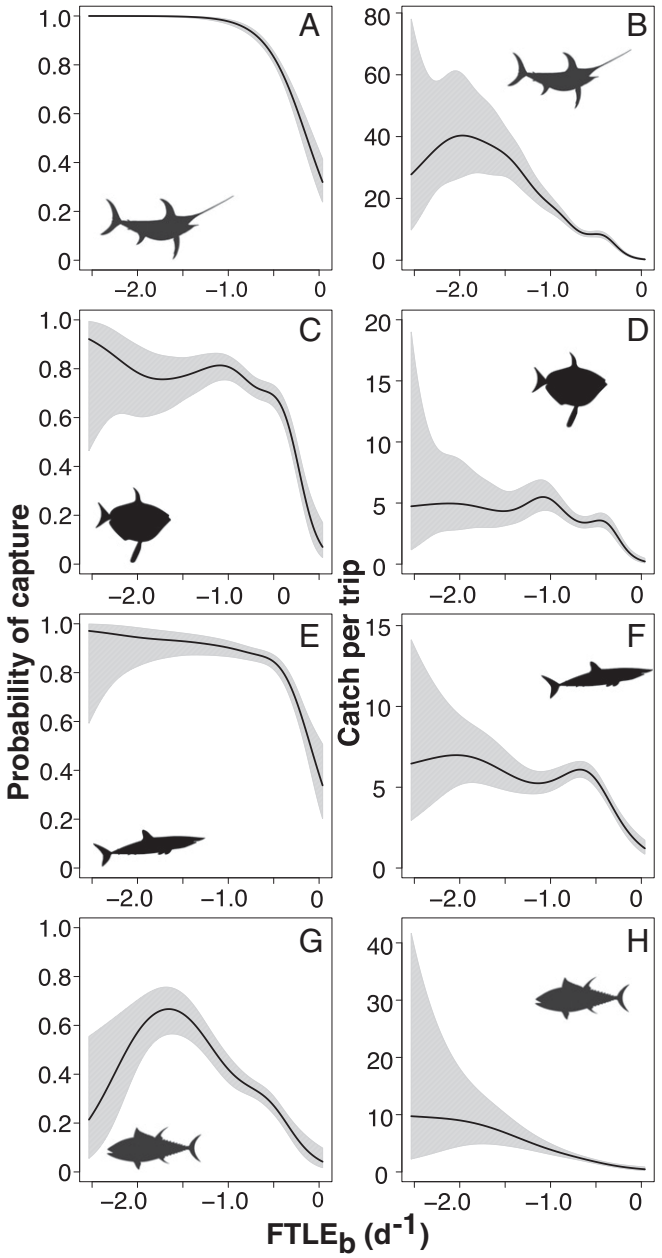

Fig. 2. Effect of FTLE$_b$ on probability of capture (*A*, *C*, *E*, and *G*) and catch per trip (*B*, *D*, *F*, and *H*) of target or secondary target species, (*A* and *B*) broadbill swordfish, (*C* and *D*) opah, (*E* and *F*) shortfin mako shark, and (*G* and *H*) bluefin tuna. Higher magnitude of negative FTLE$_b$ indicates number and strength of attracting Lagrangian coherent structures in the vicinity of each gillnet set. Shaded gray polygons show 95% confidence intervals.

caretta, California sea lion *Zalophus californianus*, northern elephant seal *Mirounga angustirostris*).

We found a highly significant influence of FTLE magnitude on swordfish catch probability (Fig. 2 *A* and *B* and *SI Appendix*). Swordfish were more likely to be caught in drift gillnets, and in higher numbers, when sets were associated with attracting LCS. Other predatory fishes including economically valuable, and vulnerable, Pacific bluefin tuna, several species of shark (common thresher, pelagic thresher, shortfin mako, smooth hammerhead, blue shark), opah, and ocean sunfish were landed as secondary targets or bycatch significantly more frequently, and in higher numbers, in attracting LCS (Figs. 2 and 3 and *SI Appendix*). In particular, attracting LCS strongly influenced rates of blue shark bycatch (Fig. 3 *E* and *F* and *SI Appendix*).

Moreover, our analyses revealed a pattern of increased risk of entanglement of protected species including cetaceans, sea turtles, and pinnipeds in association with attracting LCS (Fig. 4 and *SI Appendix*). While rates of marine megafauna bycatch in the fishery have decreased substantially since the introduction in 2001 of a large-scale seasonal closure designed to reduce sea turtle bycatch (the Pacific Leatherback Conservation Area), the observed pattern of increased bycatch likelihood of attracting LCS held true for the protected marine vertebrate group including sea

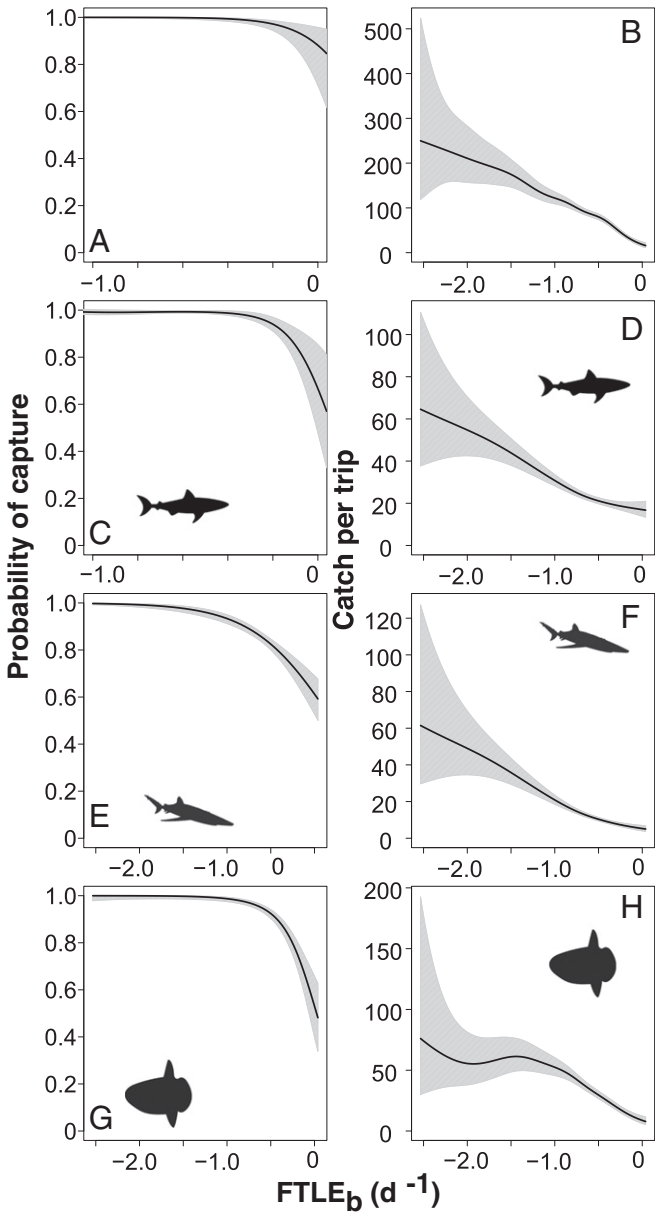

Fig. 3. Effect of FTLE$_b$ on probability of incidental capture and predicted bycatch densities of nontarget pelagic fish species. Taxon-specific probability of bycatch (*A*, *C*, *E*, and *G*) and total bycatch per trip (*B*, *D*, *F*, and *H*) for (*A* and *B*) all bycatch species, (*C* and *D*) all shark species, (*E* and *F*) blue shark, and (*G* and *H*) ocean sunfish. Higher magnitude of negative FTLE$_b$ indicates number and strength of attracting Lagrangian coherent structures in the vicinity of each gillnet set. Shaded gray polygons show 95% confidence intervals.

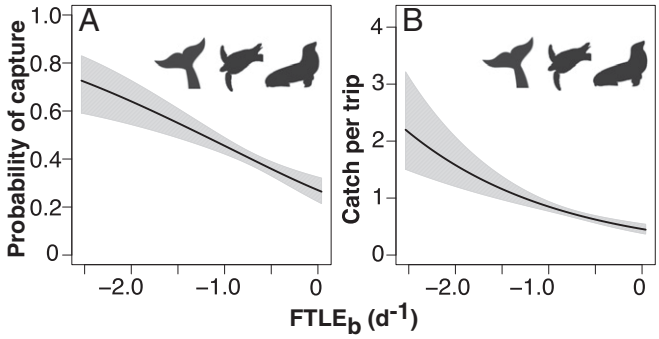

Fig. 4. Effect of $FTLE_b$ on (*A*) probability of incidental capture of protected species (cetaceans, sea turtles, pinnipeds) and (*B*) total bycatch of protected species per trip. Higher magnitude of negative $FTLE_b$ indicates number and strength of attracting Lagrangian coherent structures in the vicinity of each gillnet set. Shaded gray polygons show 95% confidence intervals.

turtles, such as the endangered loggerhead and critically endangered leatherback turtles, cetaceans listed under the Marine Mammal Protection Act (MMPA 1972) such as sperm whales *Physeter macrochephalus*, humpback whales *Megaptera novaeangliae*, beaked whales and delphinids, and MMPA-listed northern elephant seals *M. angustirostris*.

Comparing probabilities of capture and predictions of total catch across the range of species with which the fishery interacted over the 21-y study period (Figs. 2–4 and *SI Appendix*) yields valuable information regarding which species are more at risk in association with the bycatch hotspots in LCS. For example, our models predict catch rates of 40 swordfish, 60 blue shark, 75 mola, and 10 bluefin tuna per fishing trip, associated with intense LCS fields (Figs. 2 and 3). Bluefin tuna are less likely to be caught than swordfish, blue shark, or mola, but have considerably higher economic value and conservation interest.

Discussion

Given the pressing need to reduce bycatch while maintaining fisheries profitability, understanding the role of the dynamic physical environment in structuring the distributions of marine megafauna is essential in designing sustainable fisheries solutions. Our results provide an objective demonstration of the effect of (sub)mesoscale LCS in the spatial structuring of marine ecosystems and, hence, fisheries bycatch interactions. The established mechanistic function of (sub)mesoscale structures in aggregating low trophic level organisms (33–35, 55) suggests that the observed intensification of bycatch risk in LCS is mediated through regulation of forage resource availability for marine predators of both exploited and protected status.

In contrast with previous work documenting long-term, broad-scale patterns of overlap between fisheries and core habitats of marine vertebrates (23, 24, 29, 41), this study uses high-resolution Lagrangian products time-matched with spatially explicit fisheries data to quantify the influence of (sub)mesoscale structures on fisheries effort, catch rates, and the likelihood of marine vertebrate bycatch events across multiple taxa. Our approach focuses on the biophysical processes that underlie fisheries interactions, yielding important insights into the influence of the contemporaneous physical environment at spatial and temporal scales that are relevant to the design of conservation and management initiatives, particularly in developing tools for spatially dynamic ocean management (56–60).

Importantly, we find evidence of intensified likelihood of fisheries interactions in attracting LCS that holds true for target species, secondary targets, and bycatch-sensitive species. Catch rates of a diverse array of species, including elasmobranchs of management concern (e.g., blue shark, shortfin mako, common thresher, pelagic thresher), large teleost fish such as bluefin tuna, opah, and *M. mola*, and of protected species including cetaceans, sea turtles, and pinnipeds, are higher in association with LCS. Our analyses indicate that these are not coincidental interactions, as gillnet set locations are strongly associated with attracting LCS. Communication with the fisher community supports the hypothesis that the fishery actively targets (sub)mesoscale surface structures, which can be indicated by lines of advected drifting foam and debris at the surface. Some LCS are also coincident with SST discontinuities that are visible in satellite imagery, although many features do not have a signature in SST. A strategy of targeting attracting LCS appears to be profitable in that it increases the probability of catching greater numbers of the target species (see also ref. 38), but may in fact be counterproductive in also increasing the likelihood of interactions with protected species, which the fishery seeks to avoid.

Our findings suggest that including derived ocean features such as LCS in the design of dynamic ocean management solutions could facilitate bycatch reduction in marine fisheries (57). For example, dynamic time-area closures could track regions of intense submesoscale variability, such as persistent frontal zones (32), or areas in which attracting LCS manifest frequently, such as the peripheries of eddies and upwelling filaments. However, developing effective spatial tools for fisheries sustainability relies upon a knowledge of the factors that delineate and separate the distributions of target and nontarget species (44). In data-rich systems such as the CCS, using species distribution models (SDMs) that can resolve the relative distributions of target and nontarget species can inform fisheries of resource distributions and facilitate separation of catch and bycatch hotspots (40, 58, 59). Including LCS as predictors in these SDMs has potential to enhance predictive capabilities for separating fine-scale habitat preferences of target and bycatch-sensitive species, particularly where species-specific mechanistic responses to the contemporaneous physical environment are considered explicitly. Our multispecies quantification of catch and bycatch probabilities enables the development of preferential catch–bycatch strategies based on near real-time environmental conditions (see also ref. 59).

Alongside dynamic time-area closures, fine-scale set positioning with respect to LCS, as well as gear modifications for depth selectivity, could allow for continued exploitation of aggregations of target species while reducing bycatch risk. For example, the observed functional responses of tunas to submesoscale thermal fronts establishes that teleost fish are likely to be closer to the surface when exploiting thermal resources on the warm side of a front, and deeper in the water column when targeting forage resources on the cold side (47). This suggests that a strategy targeting surface aggregations on the warm side of a convergent front could avoid interactions with other nontarget endothermic predators exploiting the same bait fish aggregation near the thermocline beneath the cooler side of the front.

Vertical niche separation also confers opportunity for fine-scale selectivity through the targeting of particular depth ranges, as pelagic habitats are structured over three dimensions. Dissimilar foraging ecology, physiological constraints, and diel vertical migratory behavior influence the use of the water column by different species and age classes of large pelagic fish (61). For example, whole-body endothermy in opah allows the fish to remain in deeper, colder water for extended periods (62), whereas poikilotherms with organ-specific countercurrent heat exchange such as tuna and swordfish are more sensitive to thermal constraints and appear to use thermal fronts to maximize energetic efficiency in foraging (47). Moreover, air-breathing endotherms such as marine mammals and seabirds exhibit divergent depth utilization strategies to those of true pelagics such as sharks and large teleost fishes. Depth utilization by air-breathing predators is limited by physiological constraints, which necessitate regular dives interspersed by forays to the surface to breathe. Therefore, it would be reasonable to expect species-specific patterns of depth utilization around (sub)mesoscale structures, which could be exploited to target

certain species while avoiding others. Indeed, vertical niche separation has informed the imposition of regulation in the California drift gillnet fishery that requires fishermen to set nets at least 10 m below the surface, in an effort to avoid interactions with air-breathing species. Further gear modifications to improve selectivity through the targeting of different depth ranges could facilitate progress toward the goal of reducing bycatch.

High-resolution, data-assimilative ocean models have vast potential to generate tools for spatial fisheries management through improved understanding of species' dynamic distributions over broad scales and in three dimensions (63). By calculating FTLE from velocity fields of a data-assimilative ocean model, we better quantify physical drivers of fishery interactions than the coarse-scale overlap analyses that precede this study. Using FTLE fields derived from regional ocean models (e.g., ROMS) has several distinct advantages over satellite-based products. Data-assimilative ocean models validate and adjust hindcasts and nowcasts using real-time satellite and in situ observations. Physical data are of higher spatial resolution (here, ROMS outputs are 0.1° compared with 0.25°) and temporal frequency (daily fields as opposed to 3-d composites) than those available from satellite altimetry. Ocean models provide full velocity fields, while only geostrophic flow can be calculated from satellite altimetry. The ocean model output includes gap-free atmospheric forcing (e.g., wind stress) and physical ocean fields (e.g., temperature, salinity, zonal, and meridional velocities) at the same resolution, enabling the construction of SDMs at management-relevant scales (63). Importantly, ocean models also resolve the full 3D ocean, allowing exploration of subsurface features and conferring opportunity to improve understanding of vertical niche separation and species-specific mechanistic responses to physical conditions.

Further studies that use ocean models to address the influence of (sub)mesoscale biophysical processes on dynamic species distributions would be highly informative in developing ecosystem-based fisheries management. For example, improving understanding of the mechanistic function of repelling LCS, and of different types of frontal systems (i.e., thermal vs. chlorophyll-a; convergent vs. divergent), could elucidate further the spatial structuring of plankton communities, dynamics of prey aggregations, and niche separation of higher trophic levels (55, 64). In turn, this would enhance our operational capacity to predict fine-scale habitat utilization by both exploited and protected marine vertebrates.

Given the complexity of the bycatch problem, a suite of complementary solutions will be necessary to support a sustainable seafood supply sufficient to meet future demand. Our results highlight the conservation and management value of understanding the mechanisms through which the physical environment structures marine species distributions. Including high-resolution Lagrangian metrics in future investigations of the spatiotemporal dynamics of marine capture fisheries, and in the development of tools for dynamic ocean management, has considerable potential for enhancing fisheries sustainability and blue growth.

Methods

The spatial distribution of attracting LCS (convergent structures) for the CCS is estimated using modeled surface ocean currents produced from an implementation of ROMS with four-dimensional variational (4D-Var) data assimilation (65). Data assimilation is used to combine the observations and the numerical model to obtain the best linear unbiased estimate of the circulation (66, 67) and accurately capture the complex ocean circulation of the CCS, which is characterized by energetic mesoscale variability and pronounced seasonal upwelling driven by alongshore wind stress and wind stress curl. We use the ROMS 4D-Var daily posterior circulation estimate at 1/10° (roughly 10 km) horizontal resolution to estimate attracting LCS as ridges of the backward-in-time FTLE ($FTLE_b$) field. We acknowledge that 10 km may appear relatively coarse compared with the spatial scales of fishing. However, FLTE has been shown to be surprisingly robust to noise and low spatial resolution velocity fields (68). FTLE measures the maximum separation of close-by particles of a time-dependent flow field after a fixed, finite particle advection time. Large FTLE values identify regions where the stretching induced by mesoscale and submesoscale activity is strong and are typically organized in convoluted lines encircling submesoscale filaments. A ridge (line of local maxima) in the FTLE field can be used to predict passive tracer fronts induced by horizontal advection and stirring. Those lines have been shown to contribute to the structuring of marine ecosystems (36, 37, 48). In this study, we compute FTLE on a regular grid with 0.0125° horizontal resolution (~1 km). The final separation is computed as the maximum separation after a particle advection time of 10 d, which is the typical mesoscale eddy-turnover time in the region.

Fisheries effort was determined using data from the NOAA Fisheries Onboard Observer Program for the drift gillnet fishery. Fisheries observers recorded the location and time of haul-out of 7,996 gillnet sets deployed over a total of 1,357 fishing trips during the drift gillnet operating seasons (May–January) of 1990–2010 and coincident catch and nontarget catch data for each set. Observer coverage rates over this period are estimated at 15%. Fishing trips started from 28 ports along the US West Coast, with the majority of vessels docking in Southern California (San Diego: 51%, Morro Bay: 12%, Los Angeles: 8%; see ref. 63).

We explored the distribution of fisheries effort in relation to LCS by comparing the locations of gillnet sets with unfished locations sampled using random walkers parameterized to vessel movements. We compared the strength of the LCS field in the proximity (median over a 3- × 3-pixel radius; grid resolution 0.0125°) of each set location (presence) with that surrounding a location that was available to, but not actively targeted by, that fishing vessel on the same day (absence). These absence locations were generated using a randomization procedure based on random walkers parameterized using the distributions of departure angles, distances from port to the first set, turning angles, and distances between successive sets from all vessels that used that matching port. We generated five sets of simulated absences and iteratively resampled from this full presence–absence dataset to fit a binomial generalized linear model with a presence–absence response 1,000 times. All analyses were conducted using R v.3.3.1 (69).

We interrogated fisheries observer data to generate one master target catch dataset containing the locations, dates, and times of gillnet sets with and without swordfish catch and total catch for each successful set. To quantify the influence of attracting LCS on target catch, measured as (*i*) presence–absence of swordfish per set and (*ii*) the total number of swordfish caught per set, we calculated the median $FTLE_b$ over a 3- × 3-pixel window centered on each set location. We used the cumulative sum over each fishing trip to generate a single per-trip $FTLE_b$ metric, avoiding pseudoreplication at the trip level. We then used Generalized Additive Models (GAMs) to model the influence of LCS on (*i*) the probability of the presence of swordfish and (*ii*) cumulative total catch, as separate responses.

We used a binomial error family and logistic link function for presence–absence responses, and a negative binomial error family with a logarithmic link function for count responses. For count models, we used inbuilt theta estimation ("mgcv" package for R), checked models for overdispersion, and retained only models where the overdispersion metric was <1.4. Models were selected on the basis of parameter significance, percentage deviance explained, adjusted-R^2, and comparison of Aikaike's Information Criterion score against a null model of intercept-only. Model assumptions pertaining to GAMs, including normality and homogeneity of variance, were explicitly considered in model construction and checked using plots of residuals against fitted values and predictors where appropriate (70). The same protocol was applied to secondary targets of the fishery, including opah, bluefin tuna, thresher sharks, and shortfin mako sharks.

We modeled the correlation between total bycatch over each fishing trip and the sum of the strength of the attracting LCS field associated with each gillnet set in the same trip, using the same modeling protocol. We matched location and date information with the concomitant protected species catch dataset to obtain metrics of the incidence (0/1) and total catch of each nontarget species per gillnet set. Bycatch events were less frequent, and involved lower numbers, than catch rates of target species, and so we summarized the data in taxon-specific groupings for modeling (*SI Appendix*). For some species, such as blue shark *Prionace glauca* (caught in 54% of all sets, with a total catch of 21,146 in 21 y), sample sizes were sufficient to model a species-specific response. The rare nature of bycatch events involving protected marine vertebrates resulted in low taxon-specific sample sizes, so we combined all protected cetaceans, sea turtles, and pinnipeds into a single group for analysis.

ACKNOWLEDGMENTS. We thank two anonymous reviewers for suggestions that improved the manuscript; acknowledge the ongoing cooperation of the California drift gillnet fishery and NOAA fisheries observers; and thank

satellite data providers and data servers (NOAA CoastWatch Environmental Resource Division Data Access Portal), and University of California Santa Cruz Ocean Modeling group. Funding for this work was supplied through a National Aeronautics and Space Administration 440 Earth Science Division/ Applied Sciences Program's ROSES-2012 A.36 Ecological Forecasting Grant (NNH12ZDA001N-ECOF).

1. Dirzo R, et al. (2014) Defaunation in the anthropocene. *Science* 345:401–406.
2. Halpern BS, et al. (2008) A global map of human impact on marine ecosystems. *Science* 319:948–952.
3. Davies R, Cripps S, Nickson A, Porter G (2009) Defining and estimating global marine fisheries bycatch. *Mar Policy* 33:661–672.
4. Food and Agriculture Organisation of the United Nations (FAO) (2016) *The State of World Fisheries and Aquaculture* (FAO, Rome).
5. Smith MD, et al. (2010) Economics. Sustainability and global seafood. *Science* 327: 784–786.
6. Worm B, et al. (2006) Impacts of biodiversity loss on ocean ecosystem services. *Science* 314:787–790.
7. Pauly D, Watson R, Alder J (2005) Global trends in world fisheries: Impacts on marine ecosystems and food security. *Philos Trans R Soc Lond B Biol Sci* 360:5–12.
8. Hall MA, Alverson DL, Metuzals KI (2000) By-catch: Problems and solutions. *Mar Pollut Bull* 41:204–219.
9. Wallace BP, et al. (2003) Impacts of fisheries bycatch on marine turtle populations worldwide: Toward conservation and research priorities. *Ecosphere* 4:1–49.
10. Lewison RL, et al. (2014) Global patterns of marine mammal, seabird, and sea turtle bycatch reveal taxa-specific and cumulative megafauna hotspots. *Proc Natl Acad Sci USA* 111:5271–5276.
11. Maxwell SM, et al. (2013) Cumulative human impacts on marine predators. *Nat Commun* 4:2688.
12. Heithaus MR, Frid A, Wirsing AJ, Worm B (2008) Predicting ecological consequences of marine top predator declines. *Trends Ecol Evol* 23:202–210.
13. Ferretti F, Worm B, Britten GL, Heithaus MR, Lotze HK (2010) Patterns and ecosystem consequences of shark declines in the ocean. *Ecol Lett* 13:1055–1071.
14. Croxall JP, et al. (2012) Seabird conservation status, threats and priority actions: A global assessment. *Bird Conserv Int* 22:1–34.
15. Casini M, et al. (2009) Trophic cascades promote threshold-like shifts in pelagic marine ecosystems. *Proc Natl Acad Sci USA* 106:197–202.
16. Estes JA, et al. (2011) Trophic downgrading of planet Earth. *Science* 333:301–306.
17. Grantham HS, Petersen SL, Possingham HP (2008) Reducing bycatch in the South African pelagic longline fishery: The utility of different approaches to fisheries closures. *Endanger Species Res* 5:291–299.
18. Senko J, White E, Heppell S, Gerber L (2014) Comparing bycatch mitigation strategies for vulnerable marine megafauna. *Anim Conserv* 17:5–18.
19. Anderson OR, et al. (2011) Global seabird bycatch in longline fisheries. *Endanger Species Res* 14:91–106.
20. Gianuca D, Phillips RA, Townley S, Votier SC (2017) Global patterns of sex-and age-specific variation in seabird bycatch. *Biol Conserv* 205:60–76.
21. Gilman E, et al. (2008) Shark interactions in pelagic longline fisheries. *Mar Policy* 32: 1–18.
22. Lewison RL, Soykan CU, Franklin J (2009) Mapping the bycatch seascape: Multispecies and multi-scale spatial patterns of fisheries bycatch. *Ecol Appl* 19:920–930.
23. Fossette S, et al. (2014) Pan-atlantic analysis of the overlap of a highly migratory species, the leatherback turtle, with pelagic longline fisheries. *Proc Biol Sci* 281: 20133065.
24. Roe JH, et al. (2014) Predicting bycatch hotspots for endangered leatherback turtles on longlines in the Pacific Ocean. *Proc Biol Sci* 281:20132559.
25. Read AJ, Drinker P, Northridge S (2006) Bycatch of marine mammals in U.S. and global fisheries. *Conserv Biol* 20:163–169.
26. Moore JE, et al. (2009) A review of marine mammal, sea turtle and seabird bycatch in USA fisheries and the role of policy in shaping management. *Mar Policy* 33:435–451.
27. Sims M, Cox T, Lewison R (2008) Modeling spatial patterns in fisheries bycatch: Improving bycatch maps to aid fisheries management. *Ecol Appl* 18:649–661.
28. Žydelis R, et al. (2011) Dynamic habitat models: Using telemetry data to project fisheries bycatch. *Proc Biol Sci* 278:3191–3200.
29. Queiroz N, et al. (2016) Ocean-wide tracking of pelagic sharks reveals extent of overlap with longline fishing hotspots. *Proc Natl Acad Sci USA* 113:1582–1587.
30. Bost C-A, et al. (2009) The importance of oceanographic fronts to marine birds and mammals of the southern oceans. *J Mar Syst* 78:363–376.
31. Bailleul F, Cotté C, Guinet C (2010) Mesoscale eddies as foraging area of a deep-diving predator, the southern elephant seal. *Mar Ecol Prog Ser* 408:251–264.
32. Scales KL, et al. (2014) On the front line: Frontal zones as priority at-sea conservation areas for mobile marine vertebrates. *J Appl Ecol* 51:1575–1583.
33. Franks PJ (1992) Phytoplankton blooms at fronts: Patterns, scales, and physical forcing mechanisms. *Rev Aquat Sci* 6:121–137.
34. Taylor JR, Ferrari R (2011) Ocean fronts trigger high latitude phytoplankton blooms. *Geophys Res Lett* 38:L23601.
35. Bakun A (2006) Fronts and eddies as key structures in the habitat of marine fish larva: Opportunity, adaptive response and competitive advantage. *Sci Mar* 70:105–122.
36. Cotté C, et al. (2011) Scale-dependent interactions of Mediterranean whales with marine dynamics. *Geophys Res Lett* 56:219–232.
37. Cotté C, d'Ovidio F, Dragon A-C, Guinet C, Lévy M (2015) Flexible preference of southern elephant seals for distinct mesoscale features within the Antarctic circumpolar current. *Prog Oceanogr* 131:46–58.
38. Watson JR, Fuller EC, Castruccio FS, Samhouri JF (2018) Fishermen follow fine-scale physical ocean features for finance. *Front Mar Sci* 5:46.
39. Block BA, et al. (2011) Tracking apex marine predator movements in a dynamic ocean. *Nature* 475:86–90.
40. Howell EA, Kobayashi DR, Parker DM, Balazs GH, Polovina JJ (2008) TurtleWatch: A tool to aid in the bycatch reduction of loggerhead turtles Caretta caretta in the Hawaii-based pelagic longline fishery. *Endanger Species Res* 5:267–278.
41. Eguchi T, Benson SR, Foley DG, Forney KA (2017) Predicting overlap between drift gillnet fishing and leatherback turtle habitat in the California current ecosystem. *Fish Oceanogr* 26:17–33.
42. Zainuddin M, Kiyofuji H, Saitoh K, Saitoh S-I (2006) Using multi-sensor satellite remote sensing and catch data to detect ocean hot spots for albacore (Thunnus alalunga) in the northwestern North Pacific. *Deep Sea Res Part II Top Stud Oceanogr* 53:419–431.
43. Young JW, et al. (2011) The biological oceanography of the East Australian current and surrounding waters in relation to tuna and billfish catches off eastern Australia. *Deep Sea Res Part II Top Stud Oceanogr* 58:720–733.
44. Hsu AC, Boustany AM, Roberts JJ, Chang J-H, Halpin PN (2015) Tuna and swordfish catch in the U.S. northwest Atlantic longline fishery in relation to mesoscale eddies. *Fish Oceanogr* 24:508–520.
45. Lambert C, et al. (2017) How does ocean seasonality drive habitat preferences of highly mobile top predators? Part I: The north-western Mediterranean sea. *Deep Sea Res Part II Top Stud Oceanogr* 141:115–132.
46. Scales KL, et al. (2015) Identifying predictable foraging habitats for a wide-ranging marine predator using ensemble ecological niche models. *Divers Distrib* 22:212–224.
47. Snyder S, Franks PJS, Talley LD, Xu Y, Kohin S (2017) Crossing the line: Tunas actively exploit submesoscale fronts to enhance foraging success. *Limnol Oceanogr Lett* 2: 187–194.
48. d'Ovidio F, Fernández V, Hernández-García E, López C (2004) Mixing structures in the Mediterranean sea from finite-size Lyapunov exponents. *Geophys Res Lett* 31:L17203.
49. Haller G (2002) Lagrangian coherent structures from approximate velocity data. *Phys Fluids A Fluid Dyn* 14:1851–1861.
50. d'Ovidio F, De Monte S, Della Penna A, Cotté C, Guinet C (2013) Ecological implications of eddy retention in the open ocean: A Lagrangian approach. *J Phys A Math Theor* 46:254023.
51. Della Penna A, De Monte S, Kestenare E, Guinet C, d'Ovidio F (2015) Quasi-planktonic behavior of foraging top marine predators. *Sci Rep* 5:18063.
52. Tew Kai E, et al. (2009) Top marine predators track Lagrangian coherent structures. *Proc Natl Acad Sci USA* 106:8245–8250.
53. Scales KL, et al. (2017) Should I stay or should I go? Modelling year-round habitat suitability and drivers of residency for fin whales in the California current. *Divers Distrib* 23:1204–1215.
54. Della Penna A, et al. (2017) Lagrangian analysis of multi-satellite data in support of open ocean marine protected area design. *Deep Sea Res Part II Top Stud Oceanogr* 140:212–221.
55. Lévy M, Ferrari R, Franks PJS, Martin AP, Rivière P (2012) Bringing physics to life at the submesoscale. *Geophys Res Lett* 39:L14602.
56. Lewison R, et al. (2015) Dynamic ocean management: Identifying the critical ingredients of dynamic approaches to ocean resource management. *Bioscience* 65: 486–498.
57. Hobday AJ, Hartog JR (2014) Derived ocean features for dynamic ocean management. *Oceanography (Wash DC)* 27:134–145.
58. Hartog JR, Hobday AJ, Matear R, Feng M (2011) Habitat overlap between southern bluefin tuna and yellowfin tuna in the east coast longline fishery: Implications for present and future spatial management. *Deep Sea Res Part II Top Stud Oceanogr* 58: 746–752.
59. Hazen EL, et al. (2018) A dynamic ocean management tool to reduce bycatch and support sustainable fisheries. *Sci Adv* 4:eaar3001.
60. Hobday AJ, Hartog JR, Spillman CM, Alves O, Hilborn R (2011) Seasonal forecasting of tuna habitat for dynamic spatial management. *Can J Fish Aquat Sci* 68:898–911.
61. Preti A, et al. (2012) Comparative feeding ecology of shortfin mako, blue and thresher sharks in the California current. *Environ Biol Fishes* 95:127–146.
62. Wegner NC, Snodgrass OE, Dewar H, Hyde JR (2015) Animal physiology. Whole-body endothermy in a mesopelagic fish, the opah, Lampris guttatus. *Science* 348:786–789.
63. Scales KL, et al. (2017) Fit to predict? Eco-informatics for predicting the catchability of a pelagic fish in near real time. *Ecol Appl* 27:2313–2329.
64. Lowther AD, et al. (2014) Post-breeding at-sea movements of three central-place foragers in relation to submesoscale fronts in the Southern Ocean around Bouvetøya. *Antarct Sci* 26:533–544.
65. Neveu E, et al. (2016) An historical analysis of the California current circulation using ROMS 4D-Var: System configuration and diagnostics. *Ocean Model* 99:133–151.
66. Moore AM, et al. (2011) The regional ocean modeling system (ROMS) 4-dimensional variational data assimilation systems: Part I: System overview and formulation. *Prog Oceanogr* 91:34–49.
67. Moore AM, et al. (2011) The regional ocean modeling system (ROMS) 4-dimensional variational data assimilation systems: Part II: Performance and application to the California current system. *Prog Oceanogr* 91:50–73.
68. Harrison CS, Glatzmaier GA (2012) Lagrangian coherent structures in the California current system: Sensitivities and limitations. *Geophys Astro Fluid* 106:22–44.
69. R Core Team (2016) R: A Language and Environment for Statistical Computing (R Foundation for Statistical Computing, Vienna), Version 3.3.1.
70. Wood SN (2017) *Generalized Additive Models: An Introduction with R* (CRC Press, Boca Raton, FL).